Observations and Design of a New Neuromorphic Event-Based All-Sky and Fixed Region Imaging System

Nicholas Ralph, Darren Maybour, Yeshwanth Bethi and Gregory Cohen
The International Centre for Neuromorphic Systems, Western Sydney University, Sydney, Australia

August 2019

ABSTRACT

Current efforts in optical Space Situational Awareness (SSA), astronomy, and meteorology have seen success with typical Charged-Coupled Device (CCD) imaging. However, recent innovations made possible by Event-Based Cameras (EBCs) have opened new possibilities in imaging through the use of an asynchronous stream of individual change events triggered by changes in light intensity on a pixel-by-pixel basis. In this paper we demonstrate a series of experiments with EBCs employed in all-sky and fixed-region imaging systems. We explore all-sky observing with a circular fish-eye lens for a wide distorted view of the sky, and explore their use in a motorised pan-tilt mount for aerial scanning with a 12mm C-mount lens. We also examine narrow Field of View (FOV) fixed-point scenarios with an EBC mounted on a 600mm Ritchey-Chrétien telescope. Additionally, we demonstrate the robustness of the EBCs with an 8-inch Riccardi-Honders telescope mounted in an urban building, observing through a west-facing window. Our results show these configurations are robust to typically difficult observing conditions with successful detection of fast-moving objects in low earth orbit, and the detection of faint stars whilst observing a fixed region. Additionally, we demonstrate detections and resolved features of various aircraft. Finally, we captured day-time meteorological data with 360° imaging of detailed cloud morphology. Employing this new imaging paradigm in an all-sky and fixed-point imaging system successfully demonstrates the novel event-based sensing approach as a new means to robustly imaging faint, high-speed and distant objects.

1. INTRODUCTION

Critical services such as communication, navigation and imagery are provided to many nations using space-based commercial and research systems. These systems are under threat by the ever-increasing number and complexity of surrounding orbital systems, in addition to Near Earth Object (NEO), space debris and celestial objects that are outpacing current regulation and system control [3]. Any failures in these systems can seriously affect these services and therefore the safety of both crewed space missions and ground based services and infrastructure. Space Situational Awareness (SSA) is a critical step in mitigating hazards to orbital systems by monitoring threats and managing satellite traffic.

Current efforts in SSA have seen success with typical Coupled Charge Device (CCD) imaging, leveraged by their widespread use in astronomy. CCDs sensors use a conventional imaging paradigm of generating an image frame of information from every pixel based on a global exposure interval [6]. Frames generated by globally dependent pixels at a constant frame rate typically contain redundant information between frames and are prone to blurring and saturation effects. Recent innovations with a class of imaging devices known as neuromorphic silicon retinas, or Event-Based Camera (EBC), have opened new possibilities in imaging without many of the constraints of typical frame based imaging. Event-based sensors produce representations of the visual scene from an asynchronous stream of pixels events triggered by log changes in light intensity at each pixel [4]. These pixels produce frame-free data outputs with micro-second time resolution with much lower information redundancy. As a result, these sensors are less affected by motion blur, have a high temporal resolution, a wide dynamic range and are inherently power efficient whilst providing lower data rates than a conventional camera.

Recent research with the EBC have demonstrated the capabilities of event-based sensors on terrestrial telescopes for imaging Resident Space Objects (RSOs) in Low Earth Orbit (LEO) and Geostationary Orbit (GEO) [2]. In the same study, these sensors were also shown to be capable of observing astronomical objects, such as Jupiter and fainter

distant objects including Tycho 6621 and HIP50456. In addition to SSA applications, the properties of these sensors also render them beneficial to real-time aircraft imaging due to their high temporal resolution and low volume of collected data while observing a featureless sky. Similarly, background features such as cloud structure may also be imaged efficiently using the inherent edge detection output of the EBC.

In this paper, we explore the capabilities of all-sky and fixed-region EBC imaging systems to investigate the trade-off between resolution and total sky coverage. Whilst an all-sky imaging system can implement almost total coverage of the sky, we demonstrate how the current event-based sensors are unable to fully resolve many of the features that a narrower Field of View (FOV) fixed-region system can detect. Although this feature resolving power comes at the cost of coverage, the detected objects are more identifiable and their positions can be more accurately determined. However, given the high temporal resolution of the sensor, it is possible to actively move the sensor to compensate for the narrow field of view, and to therefore achieve better sky coverage. The four imaging systems we implemented demonstrate different aspects of this trade-off and their potential uses. Finally, we exhibit the capabilities and robust nature of the EBC in these different sensing configurations and observing conditions.

2. EXPERIMENT SETUP

2.1 All-Sky Imaging

This paper features two all-sky imaging systems to explore the coverage-resolution compromise through a simple fish-eye setup and a motorised pan-tilt system. The optical properties of these all-sky systems are summarised in Table 1. Both systems use the PSEE350 Asynchronous Time-Based Sensor (ATIS) camera[1]. The PSEE350 also features Active Pixel Sensing (APS), which combines asynchronous event detection with conventional frame-based intensity sampling [5]. These APS events were not used in these experiments.

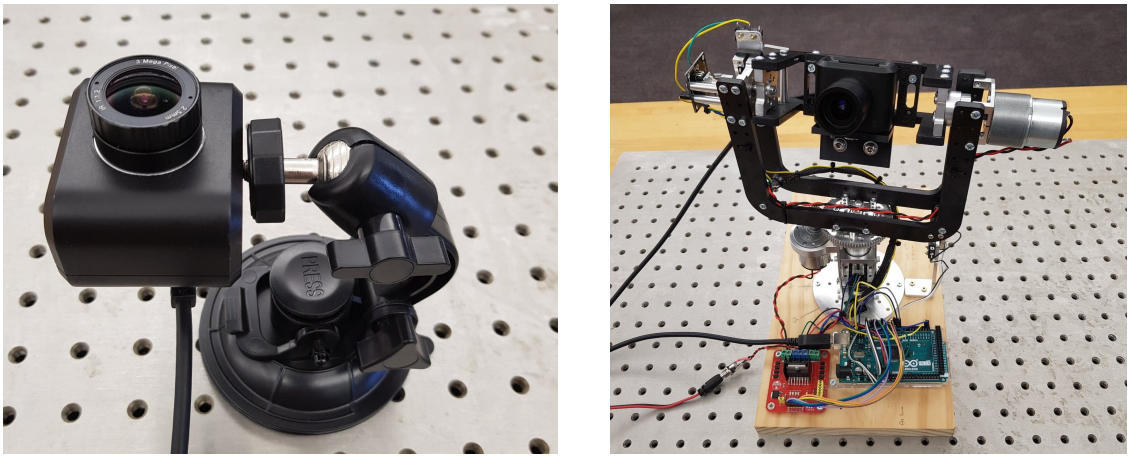

(a) (b)

Fig. 1: (a) The spherical fish-eye lens all-sky imaging setup featuring the EBC mounted on a standard suction camera mount. (b) Motorised pan-tilt mounted imaging setup featuring the EBC and mount controlled by an ATmega 2560.

2.1.1 Circular Fish-Eye Lens

The first all-sky imaging system built for this study examined the simplest approach to large FOV observing with a spherical fish-eye lens. This setup distorts the EBCs view of the hemispherical sky into a planar projection. The observing setup is shown in Fig 1 (a), where the fish-eye lens is attached to the aperture of the EBC. The EBC is mounted on a small camera mount and kept stationary throughout observing.

[1] https://www.prophesee.ai/

2.1.2 Motorised Pan-Tilt Mount

Our second all-sky imaging system compromises between resolution and coverage by physically scanning the sky with a narrower FOV than the fish-eye lens setup. As shown in Fig 1 (b), this system featured and EBC mounted on a custom-built motorised pan-tilt mount with a 12mm C-mount lens. During imaging, the pan-tilt mount performs a 360° sweep at an elevation of 30° before inclining to 60° and repeating the sweep before returning to a home position. Pointing positions are recorded with a rotary encoders connected to the shafts of the 12V DC motors driving each pan and tilt axis. During observing, this system was mounted on the roof of a car located at the Bankstown Campus of Western Sydney University with minimal obstruction of the sky.

2.2 Fixed Region Imaging

While our all-sky imaging systems were designed to observe objects and phenomenon across large regions, our fixed region imaging systems aimed to detect fainter objects and resolve more detailed features in a smaller region. These systems featured conventional telescopes pointed towards arbitrarily chosen regions of the sky for extended periods of time. The indoor Riccardi-Honders (RH) system employs the PSEE350 ATIS camera while the observatory based Ritchey-Chrétien (RC) telescope employs the PSEE300 ATIS camera. The PSEE300 does not feature APS. The optical properties of these fixed region systems are summarised in Table 1.

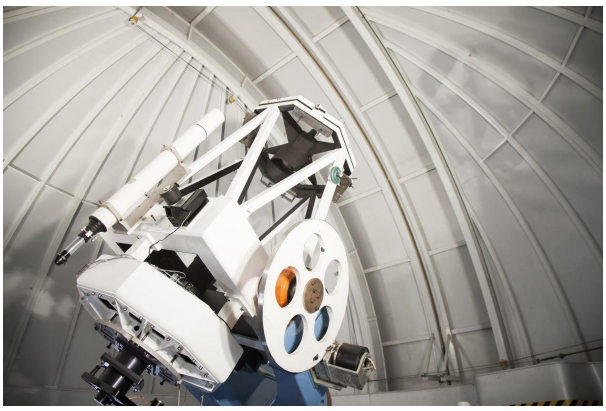

(a)

(b)

Fig. 2: (a) 600mm RC telescope housed in the Penrith Observatory dome at Western Sydney University, Werrington North Campus. (b) Indoor 8-inch RH Officina Stellare Telescope observing through a window at Western Sydney University, Werrington South Campus, Building BA Laboratory.

2.2.1 Observatory Based 600mm RC Telescope

Using a large 600mm primary mirror RC telescope shown in Fig 2 (a), we studied an extreme case of observing a small fixed region with high resolution. This was expected to provide the EBC the ability to image fainter objects and resolve finer detail than our other setups.

2.2.2 Indoor 8-inch RH Telescope

To observe a wider region, we assembled a setup shown in Fig 2 (b), featuring a wider FOV 8-inch RH telescope and EBC camera. While functioning similarly to the 600mm RC telescope, this system was intended to demonstrate the robustness of the EBC and potential urban use by observing through a west-facing window nearby to several floodlights located on the Western Sydney University, Werrington South campus. Generating a pointing model with a restricted FOV through a window proved prohibitively difficult with so few astronomical features, the pointing centre of the telescope was determined by aligning it with an identifiable star; Minelava (HIP 63090).

Imaging System	Focal Length (mm)	Focal Ratio	Primary Mirror Diameter /Aperture (mm)	FOV
Observatory Based RC Telescope	6240	f/10.3	600	7.08 $arcmin^2$
Indoor RH Telescope	1400	f/5.6	250	31.56 $arcmin^2$
Motorised Pan-Tilt Mount	12	f/1.6	11.25	56.35 deg^2
Circular Fish-Eye Lens	2.5	f/1.2	2.08	137.49 deg^2

Table 1: Specifications of optics in each imaging system

3. RESULTS

3.1 All-Sky Imaging Results

The all-sky imaging systems detailed in the Experiment Setup demonstrated greater success detecting aircraft and cloud structure than satellites. Consequently, we directed our efforts with the all-sky systems towards these applications. The pan-tilt imaging system detected small aircraft and resolved basic detail as shown in Fig 3. The high temporal resolution of the EBC results in no motion blur effects in the recordings taken with the pan-tilt mount. These aircraft were observed for a large portion of the pan-tilt sweep and are often seen through multiple passes before travelling out of view. The fish-eye setup however, lacks the feature resolving detail for either aircraft or RSOs due the poor resolution inherent from spreading such a wide FOV across a relatively low resolution detection surface. Additionally, given motion in the visual field (either from moving features or mutual motion) is required to generate events, the statically mounted fish-eye lens setup could not image the slow moving overhead cloud cover. However, the scanning motion of the pan-tilt system was sufficient to generate event changes from the edge features of overhead clouds. Fig 4 shows an image of the large and small scale structure of the overhead cloud.

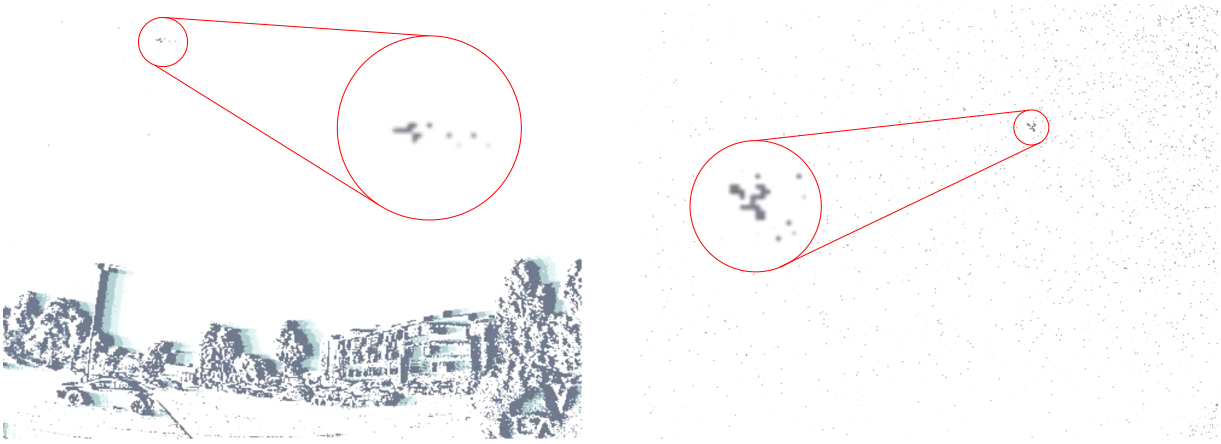

(a) (b)

Fig. 3: A small aircraft imaged with the pan-tilt system during a 30° scan (a) and the 60° scan (b). Events captured in the recording are accumulated to better show the aircraft features for display purposes. This results in the foreground features appearing blurred

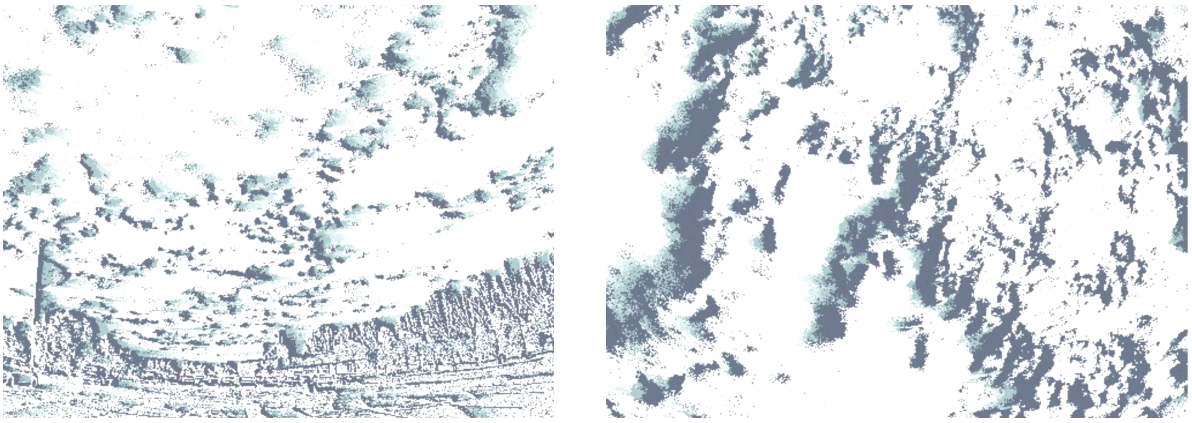

(a) (b)

Fig. 4: Segments of cloud cover image data captured using the pan-tilt mounted setup during a 30° scan (a) and the 60° scan (b). Events captured in the recording are accumulated for display purposes, causing features in foreground to blur.

3.2 Fixed-Region Imaging Results

Observing with the fixed region image systems yielded the detection of background stars, RSOs, objects in LEO and aircraft. During our experiments, the slow sidereal motion of background stars in the fixed region were sufficient to generate enough events to be imaged. The sidereal motion and speed of these objects was contrasted by the faster moving RSOs generating large volumes of events as they passed through the field. These objects can be seen in Fig 5 on the indoor RH system and the observatory based RC system in Fig 6 with RSOs producing a higher number of triggered events and a trajectory differing from the sidereal motion of the background stars. Where no motion is detected, only low volume background noise is recorded.

Aircraft in the indoor RH fixed region setup were observed during both day and night as shown in Figs 7 and 8 respectively. Day-time imaging shows resolved and recognisable features such as wings and a fuselage. Conversely, night-time imaging resolved steady and flashing external lights. Throughout observing, the indoor fixed region imaging setup also performed invariant to the effects of glare from interior lights and exterior flood lights. This performance is owed to the sensors inherent high dynamic range and event-based operation, which permits recording of only changing events not the static glare and light pollution of nearby buildings. Similar to the indoor RH setup, only noise is recorded when no objects pass through the field.

The differences found between both fixed region imaging systems were small, namely the amount of light collected due to differing apertures sizes and the FOV. Consequently, the observatory based RC telescope had a lower chance of detecting objects, but was capable of detecting fainter phenomenon and resolving more detail. This greater light collecting area is made apparent when comparing Figs 5 and 6, where the signal to noise ratio is much greater with the increased light collection and more narrow FOV of the RC setup. However, due to this narrow FOV, we did not detect any aircraft.

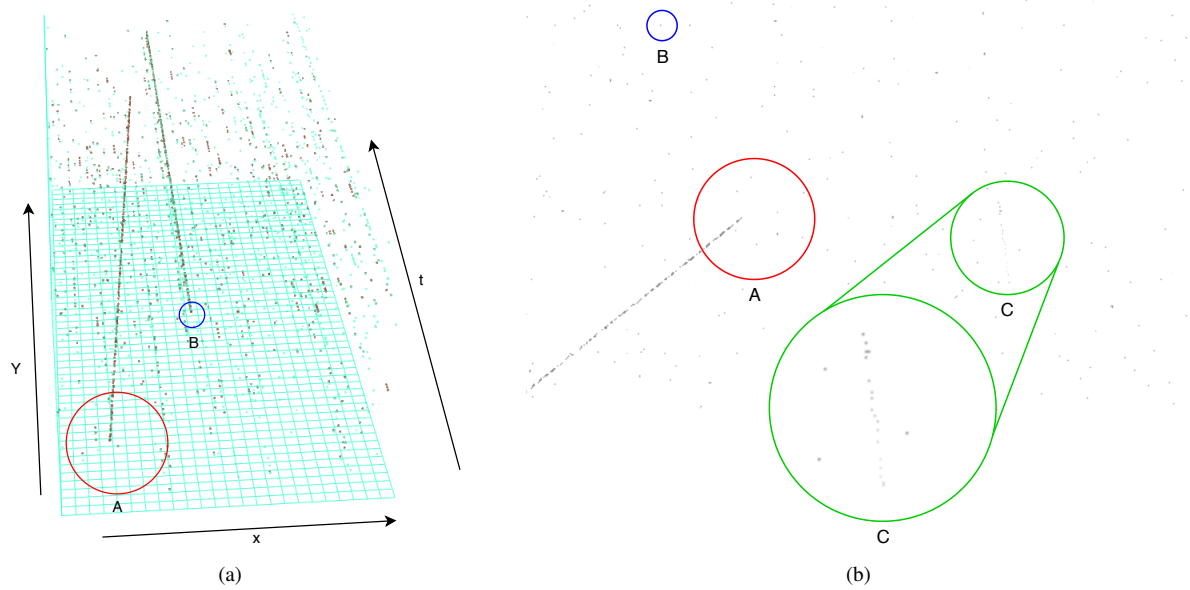

(a) (b)

Fig. 5: An unidentified RSO, Feature A (red), detected using the indoor RH setup as it passes through the fixed region. The position of the object on the sensor is shown in image (a) with 'on' (positive contrast change, maroon) and 'off' (negative contrast change, cyan) across the time axis (t). In (b), the object is displayed as accumulated events across the sensor. Feature B (blue) shows an erroneous 'hot pixel' continuously spiking throughout the recording. A faint background star generating events with its sidereal motion is annotated Feature C (green). Grid increments along the time axis, t are in 10ms intervals.

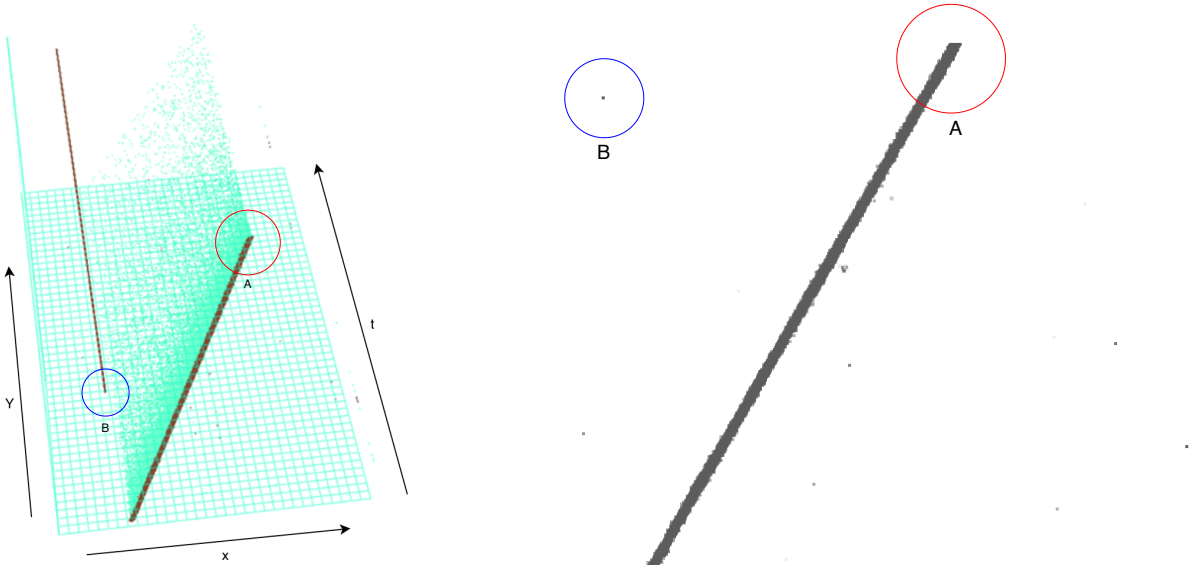

(a) (b)

Fig. 6: LEO SL-16 R/B is annotated as Feature A (red), observed from the observatory based RC setup as it passes through the fixed region. As shown in Fig 5, the position of the object on the sensor is shown in (a) across time and as accumulated events across the sensor in (b). As in Fig 5, Feature B (blue) also shows an erroneous 'hot pixel'.

Fig. 7: Unidentified aircraft observed during the day with clear morphology and features that are consistent with wings and a fuselage

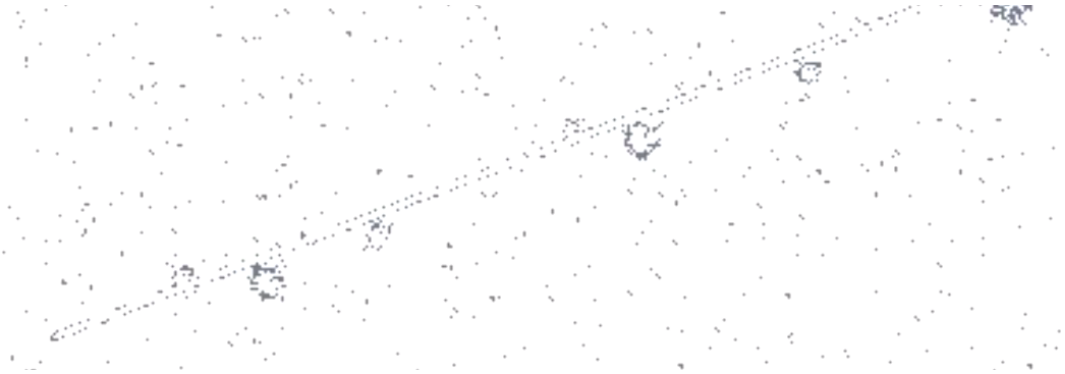

Fig. 8: Unidentified aircraft observed with during the night with features consistent with steady and flashing lights.

4. CONCLUSION

This study demonstrated the capabilities of an EBC in imaging aircraft, cloud morphology and RSOs captured from all-sky and narrow fixed region imaging systems. The novel paradigm of event-based vision and the inherent advantages of the EBC for SSA and aerial imaging were made clear by each of our imaging setups. Despite the speed of the observed objects in the fixed region systems and the mutual motion of the pan-tilt mounted system, no effects of motion blur are present in the collected event data. Moreover, the motion of the pan-tilt setup greatly increased the effective coverage of the sensor without adverse effects on the data. The robust nature of the EBC was further demonstrated with our indoor setup, which performed largely invariant to the light pollution of the surrounding urban setting and the window pane through which it was observing. The data rate of these systems is drastically lower than conventional frame based systems given the EBCs employed only gathered data on noise and small artefacts when observing a featureless sky, rather than the entire scene. Our exploration of the compromise between coverage and resolution between each imaging system was made clear by the differing capabilities of each setup. Our all-sky pan-tilt imaging system is capable of detecting aircraft and imaging cloud structure, but is largely unable to capture small features or

faint objects. This is owed to the large FOV of each lens effectively spreading the limited resolution of the EBCs detection surface over a large portion of the sky, in addition to insufficient light collection with small aperture optics. These effects are especially evident with the spherical fish-eye lens setup. We show imaging with the conventional fixed region, narrow FOV telescope can provide feature resolving capabilities on aircraft and the ability to detect RSOs with far greater aperture sizes. However, observing such a restricted region lowers the overall likelihood of observing these objects. These varying capabilities can be improved by tuning the various bias' of the EBC, such as the contrast threshold to lower the required signal at each pixel to trigger an event. This results obtained with these fixed point imaging systems indicate potential use in SSA for monitoring specific regions without the motion blur and high data rates associated with conventional cameras. Additionally, these systems show potential for use in projects such as the Desert Fireball Network, which employs a network of cameras to calculate orbits and fall positions of meteorites based on the signature 'fireball' entry through the atmosphere [1]. Future work in this area will aim to find a balance in this coverage-resolution trade-off. This would be achieved with an all-sky system featuring optics with a smaller FOV and wider aperture. Such a system would benefit from increased coverage with a fast scanning pan-tilt system and be accompanied by a direct drive telescope to slew toward detected objects and resolve fine features.

5. REFERENCES

[1] Philip A Bland. The Desert Fireball Network. *Astronomy & Geophysics*, 45(5):5.20–5.23, 10 2004.

[2] Gregory Cohen, Saeed Afshar, Andr van Schaik, Andrew Wabnitz, Travis Bessell, Mark Rutten, and Brittany Morreale. Event-based sensing for space situational awareness. 11 2017.

[3] Nicholas L Johnson, Eugene Stansbery, David O Whitlock, Kira J Abercromby, and Debra Shoots. History of on-orbit satellite fragmentations. 2008.

[4] Xavier Lagorce, Cédric Meyer, Sio-Hoi Ieng, David Filliat, and Ryad Benosman. Asynchronous event-based multikernel algorithm for high-speed visual features tracking. *IEEE transactions on neural networks and learning systems*, 26(8):1710–1720, 2014.

[5] C. Posch, D. Matolin, and R. Wohlgenannt. A qvga 143 db dynamic range frame-free pwm image sensor with lossless pixel-level video compression and time-domain cds. *IEEE Journal of Solid-State Circuits*, 46(1):259–275, Jan 2011.

[6] M. F. Tompsett, G. F. Amelio, W. J. Bertram, R. R. Buckley, W. J. McNamara, J. C. Mikkelsen, and D. A. Sealer. Charge-coupled imaging devices: Experimental results. *IEEE Transactions on Electron Devices*, 18(11):992–996, Nov 1971.